Biogeosciences Discuss., 10, 7367–7412, 2013
www.biogeosciences-discuss.net/10/7367/2013/
doi:10.5194/bgd-10-7367-2013

Biogeosciences
Discussions
Open Access

Data-based assessment of environmental controls on global marine nitrogen fixation

Y.-W. Luo[1], I. D. Lima[1], D. M. Karl[2], and S. C. Doney[1]

[1]Department of Marine Chemistry and Geochemistry, Woods Hole Oceanographic Institution, Woods Hole, Massachusetts, USA
[2]Center for Microbial Oceanography: Research and Education, University of Hawaii, Honolulu, Hawaii, USA

Received: 2 April 2013 – Accepted: 10 April 2013 – Published: 29 April 2013

Correspondence to: Y.-W. Luo (yluo@whoi.edu)

Published by Copernicus Publications on behalf of the European Geosciences Union.

Abstract

There are a number of hypotheses for the environmental controls on marine nitrogen fixation (NF). Most of these hypotheses have not been assessed against direct measurements on the global scale. In this study, we use ~500 depth-integrated field measurements of NF covering the Pacific and Atlantic Oceans to test whether the spatial variance of these measurements can be explained by the commonly hypothesized environmental controls, including measurement-based surface solar radiation, mixed layer depth, sea surface temperature, surface nitrate and phosphate concentrations, surface excess phosphate (P^*), atmospheric dust deposition and surface wind speed, as well as minimum dissolved oxygen in upper 500 m to identify possible subsurface denitrification zones. By conducting simple linear regression and stepwise multiple linear regression (MLR) analyses, solar radiation and/or sea surface temperature as well as subsurface dissolved oxygen are identified as the predictors explaining the most spatial variance in the observed NF data, while dust deposition and wind speed do not appear to influence the spatial patterns of NF on global scale. Our study suggests that marine NF is coupled to regional loss of fixed nitrogen induced by subsurface low oxygen concentration, with its magnitude constrained by solar radiation or temperature. By applying the MLR-derived equation, we estimate the global-integrated NF at 71 (error range 49–104) $\mathrm{Tg\,N\,yr^{-1}}$ in the open ocean, acknowledging that it could be substantially higher as the $^{15}N_2$-assimilation method used by most of the field samples underestimates NF. Our conclusion suggests that marine NF will increase in the future if subsurface nitrogen-losses increase as a consequence of developing deoxygenation with the global warming, a projection that will be modulated by other factors such as warming, elevated carbon dioxide, and changes in macro- and micro-nutrient distributions. More field NF samples in the Pacific and Indian Oceans, particularly in the oxygen minimum zones, are needed to reduce uncertainties in our conclusion.

BGD
10, 7367–7412, 2013

Environmental controls on marine N_2 fixation

Y.-W. Luo et al.

1 Introduction

Nitrogen (N) is one of the most important nutrients for marine ecosystems. Nitrogen fixation (NF), a process converting dinitrogen (N_2) gas into ammonia by bacteria and archaea (collectively termed diazotrophs), is considered to contribute about one half of the total input of bioavailable N into the contemporary ocean (Galloway et al., 2004; Gruber, 2008).

Marine NF has been hypothesized to be controlled by a number of environmental variables, focusing on energy and nutrient supply, as well as coupling to regional loss of fixed inorganic N (Karl et al., 2002; Deutsch et al., 2007; Carpenter and Capone, 2008; Sohm et al., 2011). Compared to assimilation of fixed forms of N such as nitrate and ammonium, NF requires additional cellular energy to split and then reduce the N_2 molecule. Thus, light can be an important factor controlling NF in supplying sufficient energy to diazotrophs (Karl et al., 2008). It has been shown that the nitrogenase (the enzymes used to fix N_2) activity of autotrophic diazotrophs is closely linked to photosynthesis (Carr and Whitton, 1982; Gallon, 2001; Karl et al., 2008). For this reason, NF generally occurs in surface seawaters with strong stratification, shallow mixed layers, and high solar energy fluxes. Enhanced stratification can also limit the resupply of nitrate into surface waters leading to fixed N stress and selection for diazotrophs. High temperature can also stimulate nitrogenase activity (Staal et al., 2003). Our current paradigm of the roles of light and temperature is supported by the fact that diazotrophs, especially *Trichodesmium*, are often found in warm marine habitats (Carpenter, 1983a,b; Carpenter and Capone, 1992), where solar energy fluxes are high and stratification is often strong. Note that marine NF by heterotrophic organisms may also be important (Halm et al., 2012) and does not directly rely on solar radiation, although the controlling mechanisms for aphotic NF are unclear but must rely on an adequate supply of energy.

Iron (Fe) and P are two major nutrients hypothesized to limit marine NF. Fe is an important cofactor for nitrogenase (Howard and Rees, 1996), and NF requires ∼5–10

BGD
10, 7367–7412, 2013
Environmental controls on marine N_2 fixation
Y.-W. Luo et al.

times more Fe than that for ammonium assimilation (Berman-Frank et al., 2001a; Kustka et al., 2003). As diazotrophs are supposedly not limited by N supply, P is inevitably another major requirement by diazotrophs. In the Atlantic Ocean, NF was reported to be limited by Fe (Moore et al., 2009; Fernández et al., 2010), by P (Sañudo-Wilhelmy et al., 2001), or co-limited by both Fe and P (Mills et al., 2004). NF in the Pacific was also reported to be controlled by Fe (Watkins-Brandt et al., 2011; Dutkiewicz et al., 2012) or P (Karl et al., 1997; Karl et al., 2001), findings which, however, were not supported by some other studies (Grabowski et al., 2008; Moutin et al., 2008).

NF may also be tied to regional loss of bioavailable N, which normally occur in subsurface oxygen minimum zones (OMZs) through denitrification (Lam and Kuypers, 2011). A low ratio of fixed N to P (< 16 : 1) in supply to the surface layer may lead to a selection for diazotrophs (Karl and Letelier, 2008). N-deficient waters can be identified by $P^*=P-N/r_n$, the excess fixed P relative to fixed N, where $r_n \approx 16$ is the average N : P in the global ocean as well as the typical N : P stoichiometry for phytoplankton biomass. Note that the P^* signal can be both a driver and a responder to marine NF: N-deficient, high P^* waters generated in subsurface layers, when brought to surface, may stimulate NF therein, which may in turn reduce the P^*. This hypothesis is supported by a geochemical model study (Deutsch et al., 2007), showing the diagnosed global marine NF estimated from transport convergence of P^* is closely tied to OMZs.

High surface wind speed can be a negative factor on NF and may lead to destratification, surface cooling and a resupply of nitrate. Furthermore, because oxygen can inhibit the nitrogenase synthesis and activity (Gallon, 1981, 1992), high wind speed has also been hypothesized to further inhibit NF by mixing atmospheric oxygen into the ocean (Howarth et al., 1993; Paerl et al., 1995). However, diazotrophs may have mechanisms to alleviate oxygen limitation (Berman-Frank et al., 2001b; Zehr, 2011), and pelagic NF is most active in the surface ocean, where dissolved oxygen concentration usually equal or exceed air saturation values. It is unlikely that bulk seawater oxygen acts as direct inhibitor to the marine NF.

Although these hypothesized environmental controls on marine NF are all plausible and may be important on both cellular and ecosystem scales, most of them have not been validated against direct field measurements on global scale. A recent effort has compiled a database, termed MAREDAT, with up-to-date direct field measurements of plankton functional groups (Buitenhuis et al., 2013), including more than 500 depth-integrated NF rates that have good spatial coverage for the tropical and subtropical Pacific and Atlantic Oceans (Luo et al., 2012). Many of these previous measurements may have significantly underestimated NF, as the $^{15}N_2$ gas used to estimate in vitro rates of NF probably does not attain equilibrium with surrounding water during a typical 12–24 h incubation period (Mohr et al., 2010). Two case studies showed that previous methods may have underestimated NF on average by ~ 40 % (Großkopf et al., 2012) and ~ 60 % (Wilson et al., 2012). However, we believe that the previous measurements can still be used to reveal spatial patterns of ocean NF. In addition, our oceanic data set represents a log-normal distribution of rates over ~ 6 orders of magnitude (Luo et al., 2012), so uncertainties of 40–60 % in measurement accuracy is probably not a first order concern in our study. In this study, we use simple linear regression and multiple linear regression (MLR) of log-transformed NF field observations to assess whether and to what degree the existing hypotheses of the environmental controls can explain observed spatial patterns of the NF in the Pacific and Atlantic Oceans. We further diagnose a globally-integrated ocean NF rate based on the resulting MLR equation, and propose how major environmental controls on NF operate in different ocean regions.

2 Methods

2.1 Data sources

NF and 9 environmental parameters were used in this study (Table 1). A total 642 depth-integrated NF rates were retrieved from the MAREDAT diazotrophic database

BGD
10, 7367–7412, 2013

(Luo et al., 2012) stored in PANGAEA (doi:10.1594/PANGAEA.774851). We only used 534 data points in the open ocean with ocean floor deeper than 250 m. None of these open ocean samples were in the Indian Ocean as the only 7 data points in the Indian Ocean were all collected in shallow coastal regions. The rates were approximately log-normally distributed (Fig. 1a and b), thus in this study we used base-10 logarithms of these rates (practically trimming 5 zero-value data points). Most rates (490 data points) were measured using $^{15}N_2$ assimilation method, and the others were based on C_2H_2 reduction. The $^{15}N_2$ assimilation method does not count the newly fixed N released by diazotrophs in dissolved forms, and may result in lower NF than those measured by the C_2H_2 reduction method (Mulholland et al., 2004; Mulholland, 2007). We included data measured by both methods in our analysis because the bias is reasonably low in log space. Furthermore, exclusion of NF rates by C_2H_2 reduction would have resulted in large data voids for regions of equatorial Pacific and subtropical Atlantic.

Assessed environmental controls included surface solar radiation, mixed layer depth, sea surface temperature (SST) (0–25 m), surface nitrate and phosphate (0–25 m), atmospheric dust deposition (representing Fe deposition), minimum dissolved oxygen in upper 500 m (representing subsurface fixed N loss) and surface wind speed (Table 1). The surface excess phosphate, P^* = phosphate – nitrate/16, was also assessed. Solar radiation and wind speed data were from the NCEP reanalysis climatology (http://www.esrl.noaa.gov/) (Kalnay et al., 1996). The nitrate, phosphate (Garcia et al., 2010b), dissolved oxygen (Garcia et al., 2010a) and temperature data (Locarnini et al., 2010) were adopted from the World Ocean Atlas 2009 (http://www.nodc.noaa.gov/). At each location, the minimum dissolved oxygen in upper 500 m was used for that location. The mixed layer depth data were downloaded from IFREMER (http://www.locean-ipsl.upmc.fr/~clement/mld.html), in which ~50 yr of in situ measurements of temperature and salinity from NODC, WOCE and ARGO programs were used to construct density profiles, and the mixed layer depth was estimated as the depth where the potential density was 0.03 kg m^{-3} higher than at the surface (de Boyer Montégut et al., 2004). For the rate of atmospheric dust deposition, we used the same product as in the Community

BGD
10, 7367–7412, 2013

Climate System Model (CCSM-3) (Doney et al., 2009): simulation of a 3-dimensional atmospheric chemical transport model which has been well validated by in situ measurements (Luo et al., 2003; Mahowald et al., 2003). The surface concentrations of nitrate, phosphate and P* and the rate of atmospheric dust deposition were approximately log-normally distributed, and thus were also log-transformed.

Annual climatologies were used for all the environmental data. They were binned on $2^\circ \times 2^\circ$ grids as most of them have original spatial resolution better than 2° (Table 1). To match the resolution, the log-transformed NF rates were also binned on $2^\circ \times 2^\circ$ grids using the mean of data in each bin, resulting in 235 binned vertically-integrated NF rates in the Pacific and Atlantic Oceans (Fig. 1c).

2.2 Regression analyses

All the regressions used in this study utilized least squares methods. Simple linear regressions were conducted for log-transformed NF against each environmental parameter. Before being applied to the regression, data were first standardized to their z-scores (Glover et al., 2011):

$$z = \frac{x - \bar{x}}{\sigma}, \quad (1)$$

where x are samples of log-transformed NF or an environmental parameter among which, again, surface nitrate, phosphate and P* and dust deposition were also log-transformed; $\bar{x}$ and σ are the mean and the standard deviation of x, respectively. We use NF_z to represent the standardized log-transformed NF hereafter. R-squared (R^2) values were calculated for each linear regression to estimate the percentage of the variance in NF_z that can be explained by each environmental parameter. We first tested regressions using only the linear, first-degree term of each environmental parameter in the regression, and then added a second-degree term (i.e. quadratic) to the regression equation.

BGD
10, 7367–7412, 2013

Stepwise multiple linear regression (MLR) analysis was conducted to establish a statistical model between NF_z and multiple standardized environmental parameters. Both first-degree and second-degree terms of all the environmental parameters were included as predictor candidates for the MLR. A stepwise procedure (Draper and Smith, 1998) iteratively added or removed predictors from the MLR model using a sequence of F tests of the change in the sum of squared errors: using p value ≤ 0.05 as a criterion to add new predictors to the model (in ascending order of p), which statistically could improve the model fit to the data; and using $p \geq 0.10$ as a criterion to remove predictors from the existing model (in descending order of p), which statistically would not deteriorate the model fit.

The final MLR equation for the fitted NF_z was:

$$NF_z = \alpha + \sum \beta_i z_i + \sum \gamma_j z_j^2, \tag{2}$$

where the first term on the right, α, is the intercept (constant term); the second term on the right is the sum of first-degree terms, with z_i representing first-degree predictors in the MLR model and β_i the corresponding coefficients; similarly, the third term in the right is the sum of the second-degree terms for the MLR predictors z_j with coefficients γ_j. Cook's distance (Cook, 1977), which measures the effect of deleting an observation from the regression, was used to identify outliers to the MLR (see Supplement). The MLR was redone after removing outliers.

We also corrected the MLR results for unreasonable terms. The last two terms in Eq. (2) were decomposed into component equations for each environmental parameter k:

$$NF_{z,k} = [\beta_k z_k] + \left[\gamma_k z_k^2\right], \tag{3}$$

where the squared brackets represent that the terms inside the brackets are included only when they were included in the MLR model. If the relation between $NF_{z,k}$ and z_k contradicts the theoretically derived direction, we noted this discrepancy, excluded that

BGD
10, 7367–7412, 2013

environmental parameter, and redid the MLR analysis. When $NF_{z,k}$ includes a second-degree term and thus the relation between $NF_{z,k}$ and z_k is not monotonic, we identified whether $NF_{z,k}$ mainly increased or decreased with z_k over the whole range.

2.3 Diagnostic estimate of global nitrogen fixation

The obtained MLR Eq. (2) was used to diagnose NF in the global ocean. To be consistent with the MLR coefficient values, the global maps of environmental parameters were transformed to z-scores using the values of mean and standard deviation found in Eq. (1) for the NF sampling locations.

In building the MLR equation, we assumed implicitly that the field data sampled NF under all the possible environmental conditions. In computing global maps we therefore needed to bound the spatial region over which the regression was valid, allowing for no extrapolation outside the domain in parameter space constrained by the regression. In the locations where NF has been observed, we calculated lower (upper) bounds for properties that correlated positively (negatively) with NF. These levels were then used as the lower (upper) limits for effective NF when estimating global NF using the MLR equation. In any location where the value of any environmental parameter included in the MLR model fell outside the limits, the estimated NF was assumed to be zero. We also limited the maximum estimated NF to the highest observed level.

For the MLR component $NF_{z,k}$ from each environmental parameter k, the spatial anomaly in the global ocean was then used to study whether that environmental parameter favored or limited NF in different ocean regions. We also compared the root mean square (RMS) of the anomalies of each component to estimate the relative contribution of each environmental parameter to the final estimated global NF.

2.4 Error propagation

For a MLR equation, considering the predicted variable as the function of the coefficients: $y = f(a_1, a_2, ..., a_n)$, the error for y, σ_y, is propagated from the covariance of the

BGD
10, 7367–7412, 2013

coefficients (Glover et al., 2011):

$$\sigma_y^2 = \sum_{i=1}^{n}\sum_{j=1}^{n}\sigma_{ij}^2\left(\frac{\partial f}{\partial a_i}\right)\left(\frac{\partial f}{\partial a_j}\right), \tag{4}$$

where σ_{ij}^2 is the covariance between coefficients i and j. Note that the covariance between a coefficient and itself, σ_{ii}^2, equals the squared error of the coefficient. Applying Eq. (4) to a MLR component Eq. (3) (if both first- and second-degree terms were included) estimates the error for $\mathrm{NF}_{z,k}$ resulting from an environment parameter k as:

$$\sigma_{\mathrm{NF}_{z},k} = \sqrt{\sigma_{\beta,k}^2 z_k^2 + \sigma_{\gamma,k}^2 z_k^4 + 2\sigma_{\beta\gamma,k}^2 z_k^3}, \tag{5}$$

where $\sigma_{\beta,k}$ and $\sigma_{\gamma,k}$ are the standard error for coefficients β_k and γ_k, respectively; $\sigma_{\beta\gamma,k}^2$ is the covariance between β_k and γ_k. Similarly, Eq. (4) was applied to the full MLR Eq. (2) to estimate the error of the fitted NF as a function of covariance of the MLR coefficients and values of environmental parameters, which were then used to estimate errors in the global estimate of NF.

3 Results

3.1 Spatial variance of nitrogen fixation and environmental parameters

The binned observations (Fig. 1c) showed different patterns of NF in the Atlantic and Pacific Oceans. Observed NF was often high in the tropical Atlantic, reaching levels on the order of 1000 μmol N m^{-2} d^{-1} in the western region. In the subtropical Atlantic, the observed NF was very low, generally on the order of 1 μmol N m^{-2} d^{-1} or less. Although the coverage in the Pacific was not as good as the Atlantic, the observed NF in the

BGD
10, 7367–7412, 2013

Pacific varied less and was mostly on the order of 10–100 µmol N m^{-2} d^{-1}, substantially higher than those found in the subtropical Atlantic.

The physical environmental parameters varied primarily with latitude with the tropics and subtropics marked by greater solar radiation, warmer SST, lower wind speeds, and shallower mixed layer depth (Fig. 2). Subsurface dissolved oxygen (< 500 m) was low in the eastern and northern Pacific and northern Indian Ocean, while in the Atlantic dissolved oxygen was low only in a small tropical region. Both the surface nitrate and phosphate concentrations were relatively low in most tropical and subtropical regions, except where high levels of nitrate and phosphate were brought up by upwelling in the eastern Pacific. This upwelling probably also brought up N-deficient waters, as shown by high surface P^* in about same region. Dust deposition was highly influenced by continental desert sources, with the highest levels in the whole tropical/subtropical North Atlantic and the Arabian Sea. In general, dust deposition was higher in the Atlantic than in the Pacific. Some of the environmental parameters were highly correlated, especially log-transformed surface phosphate and P^* ($r = 0.86$), as well as solar radiation and SST ($r = 0.71$) (Table 2).

3.2 Simple linear regression

Simple linear regressions were conducted between the standardized NF and the standardized individual environmental parameters. As discussed above, NF, nitrate, phosphate, P^* and dust deposition were log-transformed before they were standardized.

When only linear, first-degree terms were allowed for environmental parameters, the R^2 values (Table 1) showed that solar radiation explained the highest percentage (34 %) of variance in the NF. SST, minimum dissolved oxygen and mixed layer depth also explained substantial percentages of NF variance (26 %, 27 % and 19 %, respectively). The linear regression models using wind speed, surface nitrate and dust deposition statistically did not fit the observed NF well (F test, $p = 0.85$, 0.07 and 0.51, respectively). The predicted slopes (Table 1) show that the NF positively correlated to

BGD
10, 7367–7412, 2013

solar radiation and SST, and negatively correlated to mixed layer depth and minimum dissolved oxygen concentration, consistent with the hypothesized dynamics.

In many cases, the addition of a second-order, quadratic term improved the single-parameter regressions (Table 1). Allowing quadratic terms substantially increased the amount of NF variance explainable by minimum dissolved oxygen and dust deposition (Table 1). The quadratic regression model using wind speed still did not provide a good statistical fit the NF to NF (F test, $p = 0.25$). The R^2 values of the quadratic regressions against solar radiation and minimum dissolved oxygen were the highest (~ 0.4) among all the regressions. The fitted regression functions predicted that NF increased with solar radiation until reaching a saturated state (Fig. 3a). NF was high above regions with low levels of subsurface minimum dissolved oxygen and started to substantially decrease when minimum dissolved oxygen passes a certain level of $\sim 150\,\mu$M (Fig. 3b). Adding quadratic term of SST had little effect on R^2 (Table 1), predicting that NF increased approximately linearly with SST (Fig. 3c). Although the R^2 was 0.16 in the quadratic regression with atmospheric dust deposition (Table 1), the fitted function did not predict that NF increased with dust deposition (Fig. 3d), contrary to the hypothesis that Fe limited NF, assuming the required Fe was mainly supplied by dust deposition. This can actually be expected from a visual inspection of the data: dust deposition was normally lower in the Pacific than in the Atlantic (Fig. 2i), while the observed NF in most regions of the Pacific was much higher than those found in the subtropical Atlantic (Fig. 1c and d). Regionally within the Atlantic basin, NF does appear to increase with dust deposition in the field data.

3.3 Multiple linear regression

In an initial case using the first- and second-degree terms of all the environmental parameters as predictor candidates, the multiple linear regression (MLR) model included predictors of solar radiation, minimum dissolved oxygen, dust deposition, mixed layer depth, surface nitrate and wind speed, resulting in a regression equation with an R^2 value of 0.65 (Table 3). However, the resulting equation components predicted that

BGD
10, 7367–7412, 2013

NF should increase with the surface wind speed and decrease with dust deposition over ~70 % of the dust deposition range, both of which were contrary to the predicted theoretical relations (Table 3). We thus excluded individually first dust deposition and then surface wind speed from the predictor candidates in the next two cases (Table 3). When the dust deposition was excluded, the MLR did not include wind speed either, and included all the other same terms as in the initial case plus the first-degree term for P^*. When wind speed was excluded, the MLR had all the other same terms as in the initial case including the dust deposition terms, and still predicted that NF decreased with dust deposition.

In the final case used for this study, we excluded both the dust deposition and surface wind speed from the predictor candidates, which results in the same regression equation as in the case when only the dust deposition was excluded (Table 3). For this case, there was one NF rate field observation with a Cook's distance of 0.19 while all the others had values less than 0.08 (Fig. S1 in Supplement). This data point was excluded from the MLR as an outlier, which only increased the R^2 by 0.01, to 0.58 (Table 3). In this final case, the stepwise MLR (Table 4) first added the linear, first-degree term for solar radiation, which alone explained 34 % of the variance for the observed NF. The stepwise MLR then added the first- and the second-degree terms of minimum dissolved oxygen to the regression equation, increasing the R^2 value by 0.13 and thus explaining 47 % of the total variance in the observed NF. The stepwise MLR then sequentially added the first-degree term for nitrate, the second-degree term for solar radiation, and the first-degree terms for P^* and mixed layer depth, with each additional term increasing the explainable variance by ~2–4 %. The final explained variance is 58 %. The coefficients of the MLR equation, as well as the mean and standard deviation values used to standardize the data to *z*-scores, are listed in Table 5.

Mixed layer depth, nitrate and P^* contributed to the variation in the fitted NF ($\log_{10}$-transformed) by ~1 *z*-score, while minimum dissolved oxygen and solar radiation contributed by ~1.5 *z*-scores (Fig. 4). Note that as the standard deviation of the $\log_{10}$-transformed NF data is 1.1 (Table 5), one unit of change in the *z*-score roughly equals

BGD
10, 7367–7412, 2013

one order of magnitude change in the fitted NF rate. The errors associated with the individual components of the NF MLR were zero at zero z-score of the environmental parameters, increased towards larger positive/negative anomalies of the environmental parameters, and could be large where the numbers of samples were limited (Fig. 4 and Eq. 5). Note that when calculating the fitted NF, not its components, the error of intercept and the covariances among coefficients also contributed to the errors (Eq. 4), and thus the errors of the fitted NF were not zero at zero z-score of the environmental parameters. The fitted NF monotonically increased with P^* and decreased with mixed layer depth and surface nitrate (Fig. 4 and Table 3). The fitted NF component increased with solar radiation when the latter is less than zero z-score ($<\sim 230\,\mathrm{W\,m^{-2}}$) and was approximately constant at higher solar radiation (Fig. 4). The fitted NF component also decreased with minimum dissolved oxygen when the latter was higher than -1 z-score ($>\sim 90\,\mu\mathrm{M}$), stayed at a high level when the minimum dissolved oxygen ranged between -2 to -1 z-score (~ 40–$90\,\mu\mathrm{M}$) (Fig. 4). The fitted NF component slightly decreased when the level of minimum dissolved oxygen was very low (< -2 z-scores), but there are only a few samples in this range and the associated errors were large (Fig. 4). Actually, the observed NF seemed to maintain at a high level with low minimum dissolved oxygen (Fig. 3b), and thus the slight decrease of the fitted NF at low minimum dissolved oxygen in Fig. 4 was likely generated by the MLR's attempt to achieve a better overall fit, given the influence of other predictors in the MLR.

The MLR-fitted NF reproduced the general pattern of the observed NF on global scale, distributing about a 1 : 1 line (Fig. 5). Note that the MLR fitted the data from all the basins in one regression. Thus the locations of each basin's fitted data on this overall regression can tell us whether the data in that basin follow the estimated global relationships. The observed NF in the North and South Pacific distributed mostly between 0 to +1 z-score, while the MLR fitted the NF at approximately the correct order of magnitude in the North Pacific but slightly underestimated the rates in the South Pacific. Both the observed and fitted NF in the South Atlantic ranged mostly between ~ 0 to -1 z-score. The observed NF had the largest range of values in the North Atlantic,

BGD
10, 7367–7412, 2013

varying from about −3 to +2 *z*-scores. The fitted NF rates in the North Atlantic generally followed the observed pattern, but overestimated the field data when the observed rates were low and were not able to reproduce several high observed rates.

3.4 Spatial estimate of nitrogen fixation in global ocean

Following the methods discussed above, the global marine NF and the associated errors were estimated using the coefficient values from the final case MLR as well as the means and standard deviations for necessary conversions between the original units and standardized *z*-scores (Table 5). Based on the binned field data used in the MLR construction, the limits (annual climatologies) of the environmental parameters for effective NF using the MLR were: solar radiation higher than 180 $W m^{-2}$, mixed layer depth less than 75 m, surface nitrate lower than 9.4 µM, P^* higher than 0.016 µM and minimum dissolved oxygen in the upper 500 m less than 240 µM (Table 5). The maximum rate of the estimated NF was 1200 $\mu mol N m^{-2} d^{-1}$, less than the highest rate of 4700 $\mu mol N m^{-2} d^{-1}$ in the binned NF observations (Table 5).

The estimated NF (Fig. 6a) reproduced the general patterns observed in the Pacific and Atlantic, with the estimated high NF (on the order of 100 $\mu mol N m^{-2} d^{-1}$ or higher) spanning meridionaly a wider region in the Pacific than in the Atlantic. We also estimated NF for the Indian Ocean, although there are no qualified observations in this basin in the MAREDAT database to be included in the MLR. Thus practically we assumed that the NF in the Indian Ocean is controlled by the same mechanisms as those in the Pacific and Atlantic, which resulted in high estimated NF in most regions north of ∼15° S in the Indian Ocean. The environmental parameters limited effective estimated NF in the range of ∼40° S to 40° N in all the basins. The errors of the estimated NF rates (Fig. 6b) were small in most regions with the errors for the log-transformed rates mostly less than 0.2. An exception was the eastern tropical Pacific where the errors for the log-transformed rates can be higher than 0.4. The high errors in this region were mostly due to low levels of minimum dissolved oxygen (Fig. 2e) and large uncertainties in the MLR equation when the minimum dissolved oxygen was low (Fig. 4). The

BGD
10, 7367–7412, 2013

total NF in the global ocean was estimated at 71 (error range of mean ± one standard error: 49–104, same hereafter) $Tg\,N\,yr^{-1}$, comprising 12 (8.4–16), 38 (25–57) and 21 (15–31) $Tg\,N\,yr^{-1}$ in the Atlantic, Pacific and Indian Oceans, respectively (Table 6).

The environmental parameters included in the MLR model contributed to the estimated global marine NF differently. Minimum dissolved oxygen in upper 500 m contributed the most variance to the estimated global marine NF (Figs. 7a and 8). It largely set the narrow meridional range of high NF in the Atlantic. The solar radiation contributed the second highest variance to the estimated NF (Figs. 7b and 8), limiting the presence of the estimated NF to the range of ~40° S to 40° N, as the annual average solar radiation outside this range (Fig. 2a) is mostly lower than the set limit of 180 $W\,m^{-2}$ (Table 5). The upwelling in the eastern tropical Pacific led to high levels of surface nitrate, which limited the estimated NF in this region (Fig. 7c). The mixed layer depth favored NF in most tropical regions (Fig. 7d). The P^* variable favored NF in a vast region in the eastern Pacific, indicating upwelling of the denitrification signals in terms of elevated P^* promoted NF (Fig. 7e). In the Atlantic, P^* also limited NF in the tropical and the northern subtropical regions while favoring it in the southern subtropical regions. Thus multiple environmental parameters contributed to the estimated NF in a region, often in an opposing fashion. For example, in the eastern tropical Pacific, the largest positive contributions by the minimum dissolved oxygen and P^* were only partially compensated by negative contributions by nitrate. Surface nitrate may have acted as a suppressor in the MLR, which will be discussed later.

4 Discussion

4.1 Environmental controls on marine nitrogen fixation

In this study, we used several regression methods to assess hypothesized environmental controls on marine NF on the global scale using a newly compiled database of field NF measurements. Coastal samples were excluded and more than 500 depth-integrated NF rates in the open ocean were binned into 234 $2^\circ \times 2^\circ$ boxes, covering the Pacific and Atlantic Oceans, but unfortunately not the Indian Ocean. Annual climatologies of environmental parameters from different sources, mostly based on observations or modeled results validated by observations, were used in the regressions. Although we assessed multiple environmental parameters based on data availability, there can be other parameters that are currently unavailable but which could possibly also control marine NF, such as diazotrophic biomass, subsurface iron, and the fluxes of nitrate and phosphate (rather than their concentrations). Recent laboratory studies, for example, suggest that NF rates for some marine microbial diazotrophs increase with rising aqueous CO_2 concentration and that there are positive synergistic effects between elevated CO_2 and warming (Hutchins et al., 2009).

Using the simple linear regressions, we computed the variance in the observed NF explained by each individual environmental parameter. The total variance explained by the MLR using all of the environmental parameters simultaneously may differ from the sum of the R^2 values from the simple, individual-parameter linear regressions, as correlations unavoidably exist among different environmental parameters (Table 2). Part or all of the explained variance by one environmental parameter may already be covered by its correlation with other environmental parameter(s) included into the regression. The stepwise MLR represented an effort to explain the maximum variance in the observed NF with the minimum number of predictors in the final regression equation as possible. An environmental parameter may be correlated with NF but absent from the stepwise MLR, indicating that the variance that could be contributed by this parameter has been fully covered by other parameter(s).

The minimum dissolved oxygen in the upper 500 m and surface solar radiation (or SST, which is substantially correlated with solar radiation) are likely the most important environmental controls for the global spatial patterns of marine NF. These two parameters have the highest R^2 ($\sim 40\,\%$) in the simple linear regressions (Table 1). They were also the first added parameters by the stepwise MLR, explaining 47 % of the total variance even before the inclusion of the second-degree term for solar radiation (step

3 in Table 4). When the resulting MLR equation was used to map global spatial distributions, the minimum dissolved oxygen largely determined the patterns of marine NF, such as low rates in the subtropical Atlantic and high rates in the Pacific (Fig. 7a). The solar radiation mainly acted as a "mask" to limit the presence of NF to the tropical and subtropical regions; SST could have played the same role. However, the MLR component from solar radiation is mostly saturated for NF in these regions (Fig. 7b) and thus does not contribute much variance.

Linear first-degree terms from the mixed layer depth, surface nitrate and P^* were also included in the stepwise MLR model, but each of them could only explain an additional ~2–4 % of variance after the minimum dissolved oxygen and solar radiation were included in the MLR. The simple linear regression for the first-degree nitrate term explained only a low amount of variance, about 1 % (Table 1), while including the same term added a higher amount of explained variance, about 4 %, to the stepwise MLR (step 4 in Table 4). This showed that the surface nitrate acted as a suppressor for the MLR: it contributed to the explained variance indirectly by removing variance introduced by the minimum dissolved oxygen and the solar radiation. Note that ammonium concentration can be comparable or higher than that of nitrate in certain ocean regions. DON is another potential pool to supply fixed N to the ecosystem (e.g. Karl et al., 1997). The map of bioavailable N may be different if these two pools of fixed N could be included in addition to the nitrate pool. Unfortunately, there are no global coverage of measurements for ammonium and DON (particularly the bioavailability of DON).

SST was not included in the MLR model, although the simple linear regression for SST showed a relatively high R^2 of 0.27 (Table 1). This was mainly because of the high correlation (0.71) between solar radiation and SST (Table 2). When the solar radiation is removed from the predictor candidates, the stepwise MLR model includes the first- and second-degree terms of the SST and achieves a similar R^2, with all the other terms the same as the case with the solar radiation plus an additional term of second-degree P^* (Table 3). The coefficients for the other parameters and the contributions

BGD
10, 7367–7412, 2013

Title Page
Abstract | Introduction
Conclusions | References
Tables | Figures
◂◂ | ▸▸
◂ | ▸
Back | Close
Full Screen / Esc
Printer-friendly Version
Interactive Discussion

to the spatial regression patterns (not shown) remain roughly similar to the values found for the solar radiation based regression. Because of the strong spatial correlation between SST and solar radiation, we cannot use regressions alone to determine the actual underlying mechanism. Distinguishing between the two environmental factors is not necessary for globally mapping NF, but discrimination at a process level becomes more relevant, for example, in attempts to project future changes in NF in response to climate change and SST warming (Boyd and Doney, 2002; Moore et al., 2013). While the surface solar radiation is not expected to change dramatically projected surface warming could expand poleward the zonal range of NF and thus influence the global integral; a complete analysis, however, would also need to take into account other factors such as macro- and micro-nutrients and changes in subsurface oxygen.

Iron is a widely hypothesized environmental control on the spatial patterns of marine NF. In this study, we used dust deposition as a proxy for iron supply. However, the study did not show that NF increased with dust deposition when it was included in the equations for either a simple linear regression or stepwise MLR against the global data set. There is some evidence from the MAREDAT for an increase in NF with dust deposition at least regionally in the North Atlantic (Fig. 3d), but this does not appear to hold when lower dust deposition regions are included. Although the dust deposition data we used in this study are based on a model validated against limited observations (Luo et al., 2003; Mahowald et al., 2003), they capture at least the general patterns of observed deposition rates: higher in the Atlantic mainly from the Sahara Desert, lower in the vast area of the Pacific (particularly the South Pacific) because it is remote from continents (Fig. 2i). Meanwhile, the observed NF was generally high in the Pacific, but low in the subtropical Atlantic (Fig. 1c).

This result indicates that the iron supply is saturated for the NF in most regions of the open ocean, diazotrophs have adapted to low iron environment, or the iron supplied from atmospheric dust deposition is mostly bio-unavailable and the bioavailable iron in the surface ocean is mostly supplied via other processes. For example, low dissolved Fe concentration was found in the dust-rich South China Sea, hypothetically due to

Discussion Paper | Discussion Paper | Discussion Paper | Discussion Paper |

BGD
10, 7367–7412, 2013

a lack of Fe-binding organic ligands (Wu et al., 2003). Another explanation is that the diazotrophic community in the Atlantic and Pacific Oceans may be controlled by different environmental variables, and iron limits NF in the Atlantic (Moore et al., 2009) (also see Fig. 3d). Based on the data used in this study, 30 % of the variance in the observed NF in the Atlantic can be explained by dust deposition using quadratic regression. However, minimum dissolved oxygen in upper 500 m shows nearly an opposite pattern to dust deposition in the Atlantic (Fig. 2e and i), and can explain much more variance (48 %) in the observed NF in the Atlantic. It was also found that upwelling events in the eastern equatorial Atlantic can increase NF rates in the surface waters by 2 to 7 times, suggesting the subsurface waters with low N : P ratio or rich in iron are upwelled to support higher NF (Subramaniam et al., 2013). Furthermore, when combining data from both the Atlantic and the Pacific, as discussed above, minimum dissolved oxygen in upper 500 m explained substantial variance in the observed NF, while iron is only applicable in the Atlantic. Although more evidence is needed, it is possible that the iron-controlled spatial pattern of NF found in the Atlantic is generated by subsurface dissolved oxygen.

In summary, our study suggests that within the warm, stratified, high solar radiation band in the subtropics and tropics, the major factor governing spatial variations in marine NF is the regional fixed N loss induced by low-level dissolved oxygen, which generates N-deficient waters and prompts the selection for diazotrophs. Thus the N loss through denitrification can be compensated to some extent by NF regionally. The magnitude of this compensation depends on other environmental parameters mostly solar radiation (or SST), and/or mixed layer depth. Our study using field measurements confirmed the conclusion from the geochemical study by Deutsch et al. (2007).

Our results contradict, to some extent, a number of recent global prognostic modeling studies that emphasize the role of iron and atmospheric dust deposition in modulating marine NF (e.g. Moore et al., 2006; Moore and Doney, 2007). For example, the latitudinal extent of NF is similar in the simulations of Moore and Doney (2007) and the MLR-derived extrapolation, suggesting that the model variation in diazotroph growth rate

BGD
10, 7367–7412, 2013

with temperature captures either the observed correlation with solar radiation and/or SST. Regionally both approaches agree on elevated NF in the Indian Ocean, however because of iron limitation and other factors the prognostic model predicts low values in the subtropical South Pacific and eastern subtropical/tropical Pacific in disagreement with our data-derived mapped product. These differences between the modeled and data-based spatial patterns suggest that some prognostic models may overestimate the influence of iron relative to nitrogen loss processes in OMZs.

One drawback of this conclusion is that the N-deficient waters cannot be verified by the surface excess phosphate, the P^*, which does not show same pattern as the minimum dissolved oxygen (Fig. 2e and h) and does not share substantial variance with the observed NF (Table 1). Although the P^* is largely anti-correlated to the minimum dissolved oxygen in the Pacific, it is not true in the Atlantic (particularly in its tropical and south subtropical regions). As discussed above, P^* can be both a driver and a responder to NF, and low P^* can result from high NF, which could be a possible reason for the low P^* observed in the tropical Atlantic. We also did experiments using P^* at different water depths (down to 500 m) or isopycnal depths, neither of which shared substantial variance with the observed NF. The P^* in this study only considers the inorganic forms of fixed N and P, as there are no global observations of the bioavailability of DON and DOP, and P^* with both inorganic and bioavailable organic N and P may show different patterns. In the regions without strong upwelling, surface waters may not have strong contact with waters at the depth of oxygen minimum, which could be another reason for the weak correlation between P^* and oxygen minimum. The physical transport convergence of P^* can be a better way to relate the N-deficient waters to NF (Deutsch et al., 2007), but it depends on P^* field and physical transport model. We did not use P^* convergence in this study as we tried to set up an observation-based assessment.

There could be other pathways whereby the OMZs can stimulate NF. For instance, pH is low in OMZs as oxygen is consumed to decompose organic matter and to generate CO_2 and carbonic acid. While selected laboratory experiments showed reduced pH/elevated CO_2 can increase NF (Hutchins et al., 2009), field experiments did not

BGD
10, 7367–7412, 2013

show increased NF with elevated CO_2 (Law et al., 2012). The high rate of organic matter remineralization in the OMZs may also produce iron-binding ligands and prolong the residence time of dissolved iron (Hunter and Boyd, 2007; Misumi et al., 2011, 2013), which in turn could stimulate NF in the surface waters if bioavailable iron in the surface ocean is mostly supplied from the subsurface ocean.

4.2 Uncertainties for regression and global estimate

The R^2 of the stepwise MLR is 0.58, meaning that there remains 42 % of the variance in the observed NF that cannot be explained by annual mean climatologies of the environmental parameters. First we thought that using the annual climatologies may lower the explained variance. Thus we did experiments using monthly or seasonal climatologies matched to the sampling time of the observed NF, which, interestingly, resulted in substantially lower R^2 values in the simple linear regressions and the total explained variance was less than 40 % in the stepwise MLR. This may suggest that the diazotrophs are selected to inhabit ocean regions with favorable long-term environmental conditions and fix N_2 in relatively constant rates, instead of responding quickly to seasonal variability. More data are needed to verify this finding, such as long-term measurements of marine NF in certain sites, which currently are almost entirely unavailable except for monthly measurements since 2005 at Station ALOHA in the subtropical North Pacific (Church et al., 2009).

This study used a simplified model by assuming polynomial relationships between the NF and the environmental parameters (linear and up to quadratic terms). Data that were approximately log-normally distributed were also log-transformed. However, our MLR approach would not capture more non-linear relationships between NF and environmental parameters. Regressions of nonlinear models with different predictors can be complex and beyond the scope of this study, particularly when the form of the real relationships are poorly known.

Nevertheless, the MLR explained a substantial fraction of the variance in the observed NF and provided estimates of the uncertainties as function of the included

BGD
10, 7367–7412, 2013

Environmental controls on marine N_2 fixation

Y.-W. Luo et al.

Title Page
Abstract | Introduction
Conclusions | References
Tables | Figures
◀| |▶
◀ ▶
Back | Close
Full Screen / Esc
Printer-friendly Version
Interactive Discussion

environmental parameters (Fig. 4). The uncertainties were reasonable in most conditions. When the MLR equation was applied to map global patterns and the uncertainties were propagated, high uncertainties occurred almost exclusively above the OMZ in the eastern tropical Pacific (Fig. 6b). This reflects the fact that we only have a few profiles of NF rate above major OMZs (Figs. 1, 2e and 4).

To estimate total NF in different ocean basins and in the global ocean, the study by Luo et al. (2012) did not interpolate the NF data because of the limited spatial data coverage, and estimated the total NF by directly taking the geometric means of the data (Table 6). In this study, we used the same NF data, but also took advantage of the better coverage of the environmental parameters to construct a statistical model between NF and environmental parameters before estimating total NF (Table 6). Compared to Luo et al. (2012), this study estimated a comparable or slightly lower NF for the Pacific, and a significantly higher estimate for the Atlantic. The total NF in the Atlantic is still the lowest among all the basins and may yet be underestimated based on the negative regression biases at the highest observed NF values in the North Atlantic (Fig. 5).

The estimated globally-integrated NF from this study, 71 (error range: 49–104) $\mathrm{Tg\,N\,yr^{-1}}$, is at the low end of current geochemical estimates of ~100–200 $\mathrm{Tg\,N\,yr^{-1}}$ (Galloway et al., 2004; Gruber, 2008). As most of the original NF data used in this study were measured using $^{15}N_2$ method, as discussed above, this global estimate probably represents the rate of net NF (gross NF minus release of newly fixed N). Our estimates are based on the data from the open ocean, although NF can be substantial in coastal regions (Mulholland et al., 2012). We also assumed that the samples used in this study covered all possible environmental conditions for effective NF and thus limited the estimated NF to the tropical and subtropical regions. However, a recent study found substantial NF ranging from 0.02 to 4.5 $\mathrm{\mu mol\,N\,m^{-3}\,d^{-1}}$ in the surface Canadian Arctic (Blais et al., 2012). These samples were not included in this study because their sampling environmental conditions were very different from the other samples and also they were not depth-integrated samples. But they suggest marine NF can occur in higher latitudes, which would increase the current estimates of global marine NF. Finally, as discussed above, most of the previous $^{15}N_2$-based measurements may have substantially underestimated the NF (Mohr et al., 2010; Großkopf et al., 2012; Wilson et al., 2012), and thus we can expect a higher global estimate of the NF.

5 Conclusions

This data-based study assessed different environmental controls on global marine N_2 fixation (NF) using simple and multiple linear regressions. The results suggested that marine pelagic NF is limited by either solar radiation or temperature and is largely restricted to the subtropical and tropical bands. We further conclude that NF within this regions is triggered by and compensates for regional N-loss resulting from denitrification, given the constraints from solar radiation, temperature and/or mixed layer depth. Although it is possible that other environmental parameters such as iron (represented by dust deposition) and wind speed can limit marine NF over regional scales, on the global scale they were not identified by our study to explain substantial variance in the observed spatial patterns in marine NF. Applying the multiple linear regression equation and related global coverage of environmental controls, we estimated the global NF to be ~50–100 $\mathrm{Tg\,N\,yr^{-1}}$, a value at the lower end of current geochemical estimates. It was likely that we underestimated the global NF, because we excluded NF in higher latitudes, and also because most of the NF rates used in this study were likely underestimated by using the method without fully equilibrated $^{15}N_2$ gas.

Studies of field data suggest that subsurface oxygen minimum zones (OMZs) have been expanding in the tropical Pacific and other areas because of decreasing oxygen solubility as a consequence of global warming and weak ventilation resulting from enhanced stratification (Stramma et al., 2008). If the trend of deoxygenation continues, increased N loss through denitrification can be expected. Our findings indicate that marine NF may also increase in response to upwelled N-depleted waters. It is still a question if the NF can fully compensate the increased N loss, as NF is ultimately

BGD
10, 7367–7412, 2013

limited by multiple environmental variables such as solar radiation and mixed layer depth as has been demonstrated by this study. Even though our study does not indicate that iron and other nutrients are affecting NF patterns in the contemporary ocean, they could become limiting in the future if NF were to increase in concert with the N loss. As the stratification develops with global warming, the supply of nutrients from deep waters can decrease and iron, phosphorus and vitamins may act even quicker to limit elevated NF (Moore et al., 2013). Mechanistic studies are also needed to better distinguish between temperature and solar radiation controls on the zonal extent of NF.

The spatial coverage of NF observations in the MAREDAT database currently are limited in the Pacific and especially in the Indian Ocean. Our findings need to be assessed with more extensive spatial sampling in these two important ocean basins. Particularly, there were very few samples of NF above the major OMZs, such as the eastern tropical Pacific, eastern tropical Atlantic and the northern Indian Ocean, which resulted in large uncertainties in our estimated NF in these areas. Scientists tended to sample ocean regions that were believed to be inhabited by diazotrophs. Our study, however, showed some regions that can be NF "hot" zones that have not been well sampled. We suggest that a top priority for future field sampling should include measurements of marine NF within and downstream of OMZs, and then in the other areas of the Pacific and Indian Oceans. In the future, scientists should aim to set up sites above the OMZs to monitor long-term variability of the NF and to study its relationship to the climate change. Scientists should also pursue better sampling of bioavailable iron, as well as P^* through measurements of both inorganic and organic fixed N and P.

Supplementary material related to this article is available online at: http://www.biogeosciences-discuss.net/10/7367/2013/bgd-10-7367-2013-supplement.pdf.

Discussion Paper | Discussion Paper | Discussion Paper | Discussion Paper |

BGD

10, 7367–7412, 2013

Acknowledgements. This project was supported by the NSF Center for Microbial Oceanography: Research and Education (C-MORE) (EF-0424599), an NSF Emerging Topics in Biogeochemical Cycles grant (ETBC, AGS-1020594) and the Gordon and Betty Moore Foundation. NCEP Reanalysis data were provided by the NOAA/OAR/ESRL PSD, Boulder, Colorado, USA. We thank all the scientists and crews involved in collecting field samples used in this study. Dennis McGillicuddy Jr. and Larry Anderson are thanked for their useful comments to the manuscript.

References

Berman-Frank, I., Cullen, J. T., Shaked, Y., Sherrell, R. M., and Falkowski, P. G.: Iron availability, cellular iron quotas, and nitrogen fixation in *Trichodesmium*, Limnol. Oceanogr., 46, 1249–1260, doi:10.4319/lo.2001.46.6.1249, 2001a.

Berman-Frank, I., Lundgren, P., Chen, Y.-B., Kupper, H., Kolber, Z., Bergman, B., and Falkowski, P.: Segregation of nitrogen fixation and oxygenic photosynthesis in the marine cyanobacterium *Trichodesmium*, Science, 294, 1534–1537, doi:10.1126/science.1064082, 2001b.

Blais, M., Tremblay, J.-É., Jungblut, A. D., Gagnon, J., Martin, J., Thaler, M., and Lovejoy, C.: Nitrogen fixation and identification of potential diazotrophs in the Canadian Arctic, Global Biogeochem. Cy., 26, GB3022, doi:10.1029/2011gb004096, 2012.

Boyd, P. W. and Doney, S. C.: Modelling regional responses by marine pelagic ecosystems to global climate change, Geophys. Res. Lett., 29, 1806, doi:10.1029/2001gl014130, 2002.

Buitenhuis, E. T., Vogt, M., Moriarty, R., Bednaršek, N., Doney, S. C., Leblanc, K., Le Quéré, C., Luo, Y.-W., O'Brien, C., O'Brien, T., Peloquin, J., Schiebel, R., and Swan, C.: MAREDAT: towards a World Ocean Atlas of MARine Ecosystem DATa, Earth Syst. Sci. Data Discuss., 5, 1077–1106, doi:10.5194/essdd-5-1077-2012, 2012.

Carpenter, E. J.: Nitrogen fixation by marine *Oscillatoria* (*Trichodesmium*) in the world's oceans, in: Nitrogen in the Marine Environment, edited by: Carpenter, E. J. and Capone, D. G., Academic Press, New York, 65–103, 1983a.

Carpenter, E. J.: Physiology and ecology of marine planktonic *Oscillatoria* (*Trichodesmium*), Mar. Biol. Lett., 4, 69–85, 1983b.

Carpenter, E. J. and Capone, D. G.: Significance of *Trichodesmium* blooms in the marine nitrogen cycle, in: Marine Pelagic Cyanobacteria: *Trichodesmium* and other Diazotrophs, edited by: Carpenter, E. J., Capone, D. G., and Rueter, J. G., Kluwer Academic Publishers, Dordrecht, 211–217, 1992.
Carpenter, E. J. and Capone, D. G.: Nitrogen fixation in the marine environment, in: Nitrogen in the Marine Environment, 2nd edn., edited by: Capone, D. G., Bronk, D. A., Mulholland, M. R., and Carpenter, E. J., Academic Press, London, 1197–1218, 2008.
Carr, N. G. and Whitton, B. A.: The Biology of Cyanobacteria, Univ. of California Press, , 1982.
Church, M. J., Mahaffey, C., Letelier, R. M., Lukas, R., Zehr, J. P., and Karl, D. M.: Physical forcing of nitrogen fixation and diazotroph community structure in the North Pacific subtropical gyre, Global Biogeochem. Cy., 23, GB2020, doi:10.1029/2008gb003418, 2009.
Cook, R. D.: Detection of influential observation in linear regression, Technometrics, 19, 15–18, doi:10.2307/1268249, 1977.
de Boyer Montégut, C., Madec, G., Fischer, A. S., Lazar, A., and Iudicone, D.: Mixed layer depth over the global ocean: an examination of profile data and a profile-based climatology, J. Geophys. Res.-Oceans, 109, C12003, doi:10.1029/2004jc002378, 2004.
Deutsch, C., Sarmiento, J. L., Sigman, D. M., Gruber, N., and Dunne, J. P.: Spatial coupling of nitrogen inputs and losses in the ocean, Nature, 445, 163–167, doi:10.1038/nature05392, 2007.
Doney, S. C., Lima, I., Moore, J. K., Lindsay, K., Behrenfeld, M. J., Westberry, T. K., Mahowald, N., Glover, D. M., and Takahashi, T.: Skill metrics for confronting global upper ocean ecosystem-biogeochemistry models against field and remote sensing data, J. Marine Syst., 76, 95–112, doi:10.1016/j.jmarsys.2008.05.015, 2009.
Draper, N. R. and Smith, H.: Applied Regression Analysis, Wiley-Interscience, Hoboken, NJ, 1998.
Dutkiewicz, S., Ward, B. A., Monteiro, F., and Follows, M. J.: Interconnection of nitrogen fixers and iron in the Pacific Ocean: theory and numerical simulations, Global Biogeochem. Cy., 26, GB1012, doi:10.1029/2011GB004039, 2012.
Fernández, A., Mouriño-Carballido, B., Bode, A., Varela, M., and Marañón, E.: Latitudinal distribution of *Trichodesmium* spp. and N_2 fixation in the Atlantic Ocean, Biogeosciences, 7, 3167–3176, doi:10.5194/bg-7-3167-2010, 2010.
Gallon, J. R.: The oxygen sensitivity of nitrogenase: a problem for biochemists and micro-organisms, Trends Biochem. Sci., 6, 19–23, doi:10.1016/0968-0004(81)90008-6, 1981.

BGD
10, 7367–7412, 2013
Environmental controls on marine N_2 fixation
Y.-W. Luo et al.

Gallon, J. R.: Reconciling the incompatible: N_2 fixation and O_2, New Phytol., 122, 571–609, doi:10.1111/j.1469-8137.1992.tb00087.x, 1992.
Gallon, J. R.: N_2 fixation in phototrophs: adaptation to a specialized way of life, Plant Soil, 230, 39–48, doi:10.1023/A:1004640219659, 2001.
Galloway, J. N., Dentener, F. J., Capone, D. G., Boyer, E. W., Howarth, R. W., Seitzinger, S. P., Asner, G. P., Cleveland, C. C., Green, P. A., Holland, E. A., Karl, D. M., Michaels, A. F., Porter, J. H., Townsend, A. R., and Vorosmarty, C. J.: Nitrogen cycles: past, present, and future, Biogeochemistry, 70, 153–226, doi:10.1007/s10533-004-0370-0, 2004.
Garcia, H. E., Locarnini, R. A., Boyer, T. P., Antonov, J. I., Baranova, O. K., Zweng, M. M., and Johnson, D. R.: World Ocean Atlas 2009, vol. 3: dissolved oxygen, apparent oxygen utilization, and oxygen saturation, in: NOAA Atlas NESDIS 70, edited by: Levitus, S., US Government Printing Office, Washington, D.C., 344, 2010a.
Garcia, H. E., Locarnini, R. A., Boyer, T. P., Antonov, J. I., Zweng, M. M., Baranova, O. K., and Johnson, D. R.: World Ocean Atlas 2009, vol. 4: nutrients (phosphate, nitrate, silicate), in: NOAA Atlas NESDIS 71, edited by: Levitus, S., US Government Printing Office, Washington, D.C., 398, 2010b.
Glover, D. M., Jenkins, W. J., and Doney, S. C.: Modeling Methods for Marine Science, Cambridge University Press, Cambridge, UK, 2011.
Grabowski, M. N. W., Church, M. J., and Karl, D. M.: Nitrogen fixation rates and controls at Stn ALOHA, Aquat. Microb. Ecol., 52, 175–183, doi:10.3354/Ame01209, 2008.
Großkopf, T., Mohr, W., Baustian, T., Schunck, H., Gill, D., Kuypers, M. M. M., Lavik, G., Schmitz, R. A., R.Wallace, D. W., and LaRoche, J.: Doubling of marine dinitrogen-fixation rates based on direct measurements, Nature, 488, 361–364, doi:10.1038/nature11338, 2012.
Gruber, N.: The marine nitrogen cycle: overview and challenges, in: Nitrogen in the marine environment, 2nd edn., edited by: Capone, D. G., Bronk, D. A., Mulholland, M. R., and Carpenter, E. J., Elsevier, Amsterdam, 1–50, 2008.
Halm, H., Lam, P., Ferdelman, T. G., Lavik, G., Dittmar, T., LaRoche, J., D'Hondt, S., and Kuypers, M. M. M.: Heterotrophic organisms dominate nitrogen fixation in the South Pacific Gyre, ISME J., 6, 1238–1249, doi:10.1038/ismej.2011.182, 2012.
Howard, J. B. and Rees, D. C.: Structural basis of biological nitrogen fixation, Chem. Rev., 96, 2965–2982, doi:10.1021/cr9500545, 1996.

BGD
10, 7367–7412, 2013

Howarth, R. W., Butler, T., Lunde, K., Swaney, D., and Chu, C. R.: Turbulence and planktonic nitrogen-fixation – a mesocosm experiment, Limnol. Oceanogr., 38, 1696–1711, 1993.
Hunter, K. A. and Boyd, P. W.: Iron-binding ligands and their role in the ocean biogeochemistry of iron, Environ. Chem., 4, 221–232, doi:10.1071/En07012, 2007.
Hutchins, D. A., Mulholland, M. R., and Fu, F.: Nutrient cycles and marine microbes in a CO_2-enriched ocean, Oceanography, 22, 128–145, doi:10.5670/oceanog.2009.103, 2009.
Kalnay, E., Kanamitsu, M., Kistler, R., Collins, W., Deaven, D., Gandin, L., Iredell, M., Saha, S., White, G., Woollen, J., Zhu, Y., Chelliah, M., Ebisuzaki, W., Higgins, W., Janowiak, J., Mo, K. C., Ropelewski, C., Wang, J., Leetmaa, A., Reynolds, R., Jenne, R., and Joseph, D.: The NCEP/NCAR 40-year reanalysis project, B. Am. Meteorol. Soc., 77, 437–471, doi:10.1175/1520-0477(1996)077<0437:TNYRP>2.0.CO;2, 1996.
Karl, D. M. and Letelier, R. M.: Nitrogen fixation-enhanced carbon sequestration in low nitrate, low chlorophyll seascapes, Mar. Ecol.-Prog. Ser., 364, 257–268, doi:10.3354/Meps07547, 2008.
Karl, D., Michaels, A., Bergman, B., Capone, D., Carpenter, E., Letelier, R., Lipschultz, F., Paerl, H., Sigman, D., and Stal, L.: Dinitrogen fixation in the world's oceans, Biogeochemistry, 57/58, 47–98, doi:10.1023/A:1015798105851, 2002.
Karl, D. M., Letelier, R., Tupas, L., Dore, J., Christian, J., and Hebel, D.: The role of nitrogen fixation in biogeochemical cycling in the subtropical North Pacific Ocean, Nature, 388, 533–538, 1997.
Karl, D. M., Bidigare, R. R., and Letelier, R. M.: Long-term changes in plankton community structure and productivity in the North Pacific Subtropical Gyre: the domain shift hypothesis, Deep-Sea Res. Pt. II, 48, 1449–1470, doi:10.1016/S0967-0645(00)00149-1, 2001.
Karl, D. M., Bidigare, R. R., Church, M. J., Dore, J. E., Letelier, R. M., Mahaffey, C., and Zehr, J. P.: The nitrogen cycle in the North Pacific trades biome: an evolving paradigm, in: Nitrogen in the Marine Environment, 2nd edn., edited by: Capone, D. G., Bronk, D. A., Mulholland, M. R., and Carpenter, E. J., Elsevier, Amsterdam, 705–769, 2008.
Kustka, A. B., Sanudo-Wilhelmy, S. A., Carpenter, E. J., Capone, D. G., Burns, J., and Sunda, W. G.: Iron requirements for dinitrogen- and ammonium-supported growth in cultures of *Trichodesmium* (IMS 101): comparsion with nitrogen fixation rates and iron : carbon ratios of field populations, Limnol. Oceanogr., 48, 1869–1884, doi:10.4319/lo.2003.48.5.1869, 2003.

Lam, P. and Kuypers, M. M. M.: Microbial nitrogen cycling processes in oxygen minimum zones, Annu. Rev. Mar. Sci., 3, 317–345, doi:10.1146/annurev-marine-120709-142814, 2011.
Law, C. S., Breitbarth, E., Hoffmann, L. J., McGraw, C. M., Langlois, R. J., LaRoche, J., Marriner, A., and Safi, K. A.: No stimulation of nitrogen fixation by non-filamentous diazotrophs under elevated CO_2 in the South Pacific, Global Change Biol., 18, 3004–3014, doi:10.1111/j.1365-2486.2012.02777.x, 2012.
Locarnini, R. A., Mishonov, A. V., Antonov, J. I., Boyer, T. P., Garcia, H. E., Baranova, O. K., Zweng, M. M., and Johnson, D. R.: World Ocean Atlas 2009, vol. 1: temperature, in: NOAA Atlas NESDIS 68, edited by: Levitus, S., US Government Printing Office, Washington, D.C., 184, 2010.
Luo, C., Mahowald, N. M., and del Corral, J.: Sensitivity study of meteorological parameters on mineral aerosol mobilization, transport, and distribution, J. Geophys. Res.-Atmos., 108, 4447, doi:10.1029/2003jd003483, 2003.
Luo, Y.-W., Doney, S. C., Anderson, L. A., Benavides, M., Berman-Frank, I., Bode, A., Bonnet, S., Boström, K. H., Böttjer, D., Capone, D. G., Carpenter, E. J., Chen, Y. L., Church, M. J., Dore, J. E., Falcón, L. I., Fernández, A., Foster, R. A., Furuya, K., Gómez, F., Gundersen, K., Hynes, A. M., Karl, D. M., Kitajima, S., Langlois, R. J., LaRoche, J., Letelier, R. M., Marañón, E., McGillicuddy Jr., D. J., Moisander, P. H., Moore, C. M., Mouriño-Carballido, B., Mulholland, M. R., Needoba, J. A., Orcutt, K. M., Poulton, A. J., Rahav, E., Raimbault, P., Rees, A. P., Riemann, L., Shiozaki, T., Subramaniam, A., Tyrrell, T., Turk-Kubo, K. A., Varela, M., Villareal, T. A., Webb, E. A., White, A. E., Wu, J., and Zehr, J. P.: Database of diazotrophs in global ocean: abundance, biomass and nitrogen fixation rates, Earth Syst. Sci. Data, 4, 47–73, doi:10.5194/essd-4-47-2012, 2012.
Mahowald, N., Luo, C., del Corral, J., and Zender, C. S.: Interannual variability in atmospheric mineral aerosols from a 22-year model simulation and observational data, J. Geophys. Res.-Atmos., 108, 4352, doi:10.1029/2002jd002821, 2003.
Mills, M. M., Ridame, C., Davey, M., La Roche, J., and Geider, R. J.: Iron and phosphorus co-limit nitrogen fixation in the eastern tropical North Atlantic, Nature, 429, 292–294, doi:10.1038/nature02550, 2004.
Misumi, K., Tsumune, D., Yoshida, Y., Uchimoto, K., Nakamura, T., Nishioka, J., Mitsudera, H., Bryan, F. O., Lindsay, K., Moore, J. K., and Doney, S. C.: Mechanisms controlling dissolved iron distribution in the North Pacific: a model study, J. Geophys. Res.-Biogeo., 116, G03005, doi:10.1029/2010jg001541, 2011.

BGD
10, 7367–7412, 2013

Misumi, K., Lindsay, K., Moore, J. K., Doney, S. C., Tsumune, D., and Yoshida, Y.: Humic substances may control dissolved iron distributions in the global ocean: Implications from numerical simulations, Global Biogeochem. Cy., in press, doi:10.1002/gbc.20039, 2013.

Mohr, W., Grosskopf, T., Wallace, D. W. R., and LaRoche, J.: Methodological underestimation of oceanic nitrogen fixation rates, PLoS One, 5, e12583, doi:10.1371/journal.pone.0012583, 2010.

Moore, C. M., Mills, M. M., Achterberg, E. P., Geider, R. J., LaRoche, J., Lucas, M. I., McDonagh, E. L., Pan, X., Poulton, A. J., Rijkenberg, M. J. A., Suggett, D. J., Ussher, S. J., and Woodward, E. M. S.: Large-scale distribution of Atlantic nitrogen fixation controlled by iron availability, Nat. Geosci., 2, 867–871, doi:10.1038/ngeo667, 2009.

Moore, J. K., Lindsay, K., Doney, S. C., Long, M. C., and Misumi, K.: Marine ecosystem dynamics and biogeochemical cycling in the Community Earth System Model (CESM1.0), J. Climate, submitted, 2013.

Moutin, T., Karl, D. M., Duhamel, S., Rimmelin, P., Raimbault, P., Van Mooy, B. A. S., and Claustre, H.: Phosphate availability and the ultimate control of new nitrogen input by nitrogen fixation in the tropical Pacific Ocean, Biogeosciences, 5, 95–109, doi:10.5194/bg-5-95-2008, 2008.

Mulholland, M. R.: The fate of nitrogen fixed by diazotrophs in the ocean, Biogeosciences, 4, 37–51, doi:10.5194/bg-4-37-2007, 2007.

Mulholland, M. R., Bronk, D. A., and Capone, D. G.: Dinitrogen fixation and release of ammonium and dissolved organic nitrogen by *Trichodesmium* IMS101, Aquat. Microb. Ecol., 37, 85–94, doi:10.3354/ame037085, 2004.

Mulholland, M. R., Bernhardt, P. W., Blanco-Garcia, J. L., Mannino, A., Hyde, K., Mondragon, E., Turk, K., Moisander, P. H., and Zehr, J. P.: Rates of dinitrogen fixation and the abundance of diazotrophs in North American coastal waters between Cape Hatteras and Georges Bank, Limnol. Oceanogr., 57, 1067–1083, doi:10.4319/lo.2012.57.4.1067, 2012.

Paerl, H. W., Pinckney, J. L., and Kucera, S. A.: Clarification of the structural and functional roles of heterocysts and anoxic microzones in the control of pelagic nitrogen-fixation, Limnol. Oceanogr., 40, 634–638, 1995.

Sañudo-Wilhelmy, S. A., Kustka, A. B., Gobler, C. J., Hutchins, D. A., Yang, M., Lwiza, K., Burns, J., Capone, D. G., Raven, J. A., and Carpenter, E. J.: Phosphorus limitation of nitrogen fixation by *Trichodesmium* in the central Atlantic Ocean, Nature, 411, 66–69, doi:10.1038/35075041, 2001.

Sohm, J. A., Webb, E. A., and Capone, D. G.: Emerging patterns of marine nitrogen fixation, Nat. Rev. Microbiol., 9, 499–508, doi:10.1038/nrmicro2594, 2011.
Staal, M., Meysman, F. J. R., and Stal, L. J.: Temperature excludes N_2-fixing heterocystous cyanobacteria in the tropical oceans, Nature, 425, 504–507, doi:10.1038/Nature01999, 2003.
Stramma, L., Johnson, G. C., Sprintall, J., and Mohrholz, V.: Expanding oxygen-minimum zones in the tropical oceans, Science, 320, 655–658, doi:10.1126/science.1153847, 2008.
Subramaniam, A., Mahaffey, C., Johns, W., and Mahowald, N.: Equatorial upwelling enhances nitrogen fixation in the Atlantic Ocean, Geophys. Res. Lett., in press, doi:10.1002/grl.50250, 2013.
Watkins-Brandt, K. S., Letelier, R. M., Spitz, Y. H., Church, M. J., Böttjer, D., and White, A. E.: Addition of inorganic or organic phosphorus enhances nitrogen and carbon fixation in the oligotrophic North Pacific, Mar. Ecol.-Prog. Ser., 432, 17–29, doi:10.3354/meps09147, 2011.
Wilson, S. T., Böttjer, D., Church, M. J., and Karl, D. M.: Comparative assessment of nitrogen fixation methodologies conducted in the oligotrophic North Pacific Ocean, Appl. Envir. Microbiol., 78, 6516–6523, doi:10.1128/AEM.01146-12, 2012.
Wu, J. F., Chung, S. W., Wen, L. S., Liu, K. K., Chen, Y. L. L., Chen, H. Y., and Karl, D. M.: Dissolved inorganic phosphorus, dissolved iron, and *Trichodesmium* in the oligotrophic South China Sea, Global Biogeochem. Cy., 17, 1008, doi:10.1029/2002gb001924, 2003.
Zehr, J. P.: Nitrogen fixation by marine cyanobacteria, Trends Microbiol., 19, 162–173, doi:10.1016/j.tim.2010.12.004, 2011.

BGD
10, 7367–7412, 2013

Table 1. Data sources of nitrogen fixation and environmental parameter and the simple linear regression results[a].

Data description	Symbol	Source	Spatial resolution	Log-normally distributed and log-transformed	Regression to nitrogen fixation		
					R^2 (linear)	Slope (linear)	R^2 (quadratic)
Depth-integrated nitrogen fixation (μmol N m^{-2} d^{-1})	NF	MAREDAT		Yes			
Surface downward solar radiation (W m^{-2})	LIGHT	NCEP	∼ 1.9°	No	0.34	0.58 ± 0.05	0.38
Surface wind speed (m s^{-1})	WIND	Reanalysis	2.5°	No	**0.00**[b]	−0.01 ± 0.07	**0.01**[b]
Mixed layer depth (m)	MLD	IFREMER	2°	No	0.19	−0.44 ± 0.06	0.19
Sea surface temperature (°C)	SST	World	1°	No	0.26	0.51 ± 0.06	0.27
Minimum dissolved oxygen in 0–500 m (μM)	DO_{min}	Ocean	1°	No	0.27	−0.52 ± 0.06	0.39
Surface nitrate (μM)	DIN	Atlas	1°	Yes	**0.01**[b]	−0.12 ± 0.07	0.03
Surface phosphate (μM)	DIP	2009	1°	Yes	0.03	0.16 ± 0.06	0.03
Excess phosphate (μM)	P*	DIP-DIN/16	1°	Yes	0.07	0.26 ± 0.06	0.07
Surface dust deposition (mg m^{-2} d^{-1})	DST	Model	∼ 1.9°	Yes	**0.00**[b]	−0.04 ± 0.07	0.16

[a] Regression results are for standardized log-transformed nitrogen fixation rate versus each standardized environmental parameter, including R^2 and slope (± one standard error) when only linear, 1st-degree terms were used, and R^2 when quadratic, 2nd-degree terms are added. Note that DIN, DIP, P* and DST were also log-transformed before standardization.

[b] Regression model statistically does not fit the data well, with p value of F test larger than 0.05.

BGD
10, 7367–7412, 2013
Environmental controls on marine N_2 fixation
Y.-W. Luo et al.

Table 2. Correlations among environmental parameters at the locations of nitrogen fixation data[a].

	SST	MLD	LOG_{10}(DIN)	LOG_{10}(DIP)	$LOG_{10}(P^*)$	LOG_{10}(DST)	DO_{min}	WIND
LIGHT	0.71	−0.42	−0.06	0.15	0.17	0.15	−0.56	−0.10
SST		−0.45	−0.12	−0.15	−0.12	0.29	−0.40	−0.09
MLD			−0.35	−0.14	−0.01	−0.43	0.45	0.05
LOG_{10}(DIN)				0.55	0.18	0.13	−0.31	−0.07
LOG_{10}(DIP)					0.86	−0.45	−0.50	−0.28
$LOG_{10}(P^*)$						−0.59	−0.38	−0.24
LOG_{10}(DST)							0.03	0.40
DO_{min}								0.08

[a] See Table 1 for abbreviations of environmental parameters.

Discussion Paper | Discussion Paper | Discussion Paper | Discussion Paper |
BGD
10, 7367–7412, 2013
Environmental controls on marine N_2 fixation
Y.-W. Luo et al.

Table 3. Results of stepwise multiple linear regression (MLR)[a].

	Environmental Parameters (Predictor Candidates)									R^2	RMSe
	LIGHT	SST	MLD	LOG_{10} (DIN)	LOG_{10} (DIP)	LOG_{10} (P^*)	DO_{min}	LOG_{10} (DST)	WIND		
Expected Correlation	+	+	–	–	+	+	–	+	–		
Included Predictor Candidates in MLR											
All Environmental Parameters	+ (71 %)		–	–			– (55 %)	– (71 %)	+	0.65	0.69
Exclude DST	+ (64 %)		–	–		+	– (62 %)	EX		0.57	0.76
Exclude WIND	+ (73 %)		–	–			– (55 %)	– (67 %)	EX	0.62	0.72
(Final) Exclude DST and WIND[b]	+ (64 %)		–	–		+	– (62 %)	EX	EX	0.58	0.76
Experiment:											
Exclude LIGHT, DST and WIND	EX	+ (64 %)	–	–		– (75 %)	– (54 %)	EX	EX	0.58	0.75

[a] Expected relationships between nitrogen fixation and environmental parameters are shown as positive (+) or negative (–). By including different environmental parameters as predictor candidates for the MLR, the equation shows predicted nitrogen fixation component increases (+) or decreases (–) with each included predictor. In cases where the resulted function was quadratic for a predictor, the table shows whether predicted nitrogen fixation mainly increases (+) or decreases (–) with the predictor within the range of the parameter, and the percentage of the range on which the increase or decrease was effective. Blank represents cases where the predictor was not included in the MLR model. Also shown are the R^2 and root mean square of error (RMSe) values for the MLR estimate of the log-transformed nitrogen fixation. See Table 1 for abbreviations of environmental parameters. EX: excluded.

[b] One data point was excluded because of high Cook's distance.

BGD
10, 7367–7412, 2013

Table 4. Stepwise results for the final case of the multiple linear regression (MLR)[a].

Step #	Added Term	*p* value	R^2
1	Constant term		
2	LIGHT	1×10^{-22}	0.34
3	DO_{min}	3×10^{-6}	0.40
4	$(DO_{min})^2$	5×10^{-8}	0.47
5	$LOG_{10}(DIN)$	5×10^{-5}	0.51
6	$(LIGHT)^2$	0.0006	0.53
7	$LOG_{10}(P^*)$	0.0004	0.56
8	MLD	0.0005	0.58

[a] Dust deposition and surface wind speed were excluded as predictor candidates in this case. The table shows the term added in each step, the *p* value for the *F* test for the term addition, and the R^2 values of the MLR in that step. See Table 1 for abbreviations of environmental parameters.

BGD
10, 7367–7412, 2013

Environmental controls on marine N_2 fixation

Y.-W. Luo et al.

Discussion Paper | Discussion Paper | Discussion Paper | Discussion Paper |

BGD

10, 7367–7412, 2013

Environmental controls on marine N_2 fixation

Y.-W. Luo et al.

Table 5. Final multiple linear regression (MLR) results[a].

		LIGHT ($W\,m^{-2}$)	MLD (m)	LOG_{10}(DIN) (µM)	LOG_{10}(P^*) (µM)	DO_{min} (µM)	LOG_{10}(Nitrogen Fixation) ($\mu mol\,N\,m^{-2}\,d^{-1}$)
Mean ± standard deviation of data		232 ± 16	40 ± 12	−0.51 ± 0.54	−1.1 ± 0.3	138 ± 47	1.2 ± 1.1
Intercept	0.30 ± 0.07						
Coefficient of 1st-degree term in MLR		0.062 ± 0.066	−0.21 ± 0.06	−0.25 ± 0.05	0.21 ± 0.05	−0.45 ± 0.07	
Coefficient of 2nd-degree term in MLR		−0.11 ± 0.04				−0.20 ± 0.04	
Limits[b]		> 180 $W\,m^{-2}$	< 75 m	< 9.4 µM	> 0.016 µM	< 240 µM	< 4700 $\mu mol\,N\,m^{-2}\,d^{-1}$

[a] Mean and standard deviation of data were used to standardize data to *z*-scores, which were then used in the MLR. Also shown are coefficients ± one standard error of the linear first-degree term and, if applicable, of the quadratic second-degree term of each included predictor in MLR. The limits of predictor and maximum allowed nitrogen fixation were also presented. See Table 1 for abbreviations of predictors.

[b] All numbers are in specified units without log-transform.

Table 6. Comparison of estimated spatially-integrated nitrogen fixation ($Tg\,N\,yr^{-1}$) in this study and in Luo et al. (2012)[a].

Basin	This study	Luo et al. (2012)
North Atlantic Ocean	7.5 (5.6–10)	1.7 (1.3–2.2)
South Atlantic Ocean	4.1 (2.8–6.0)	1.1 (0.9–1.4)
North Pacific Ocean	23 (15–36)	35 (30–41)
South Pacific Ocean	15 (10–21)	24 (20–28)
Indian Ocean	21 (15–31)	–
Global Ocean	71 (49–104)	62 (52–73)

[a] Estimates in this study uses the equation from the final multiple linear regression. Estimates in Luo et al. (2012) are spatially-integrated nitrogen fixation estimated from geometric means of field data in every basin. Numbers in brackets are error ranges.

BGD
10, 7367–7412, 2013

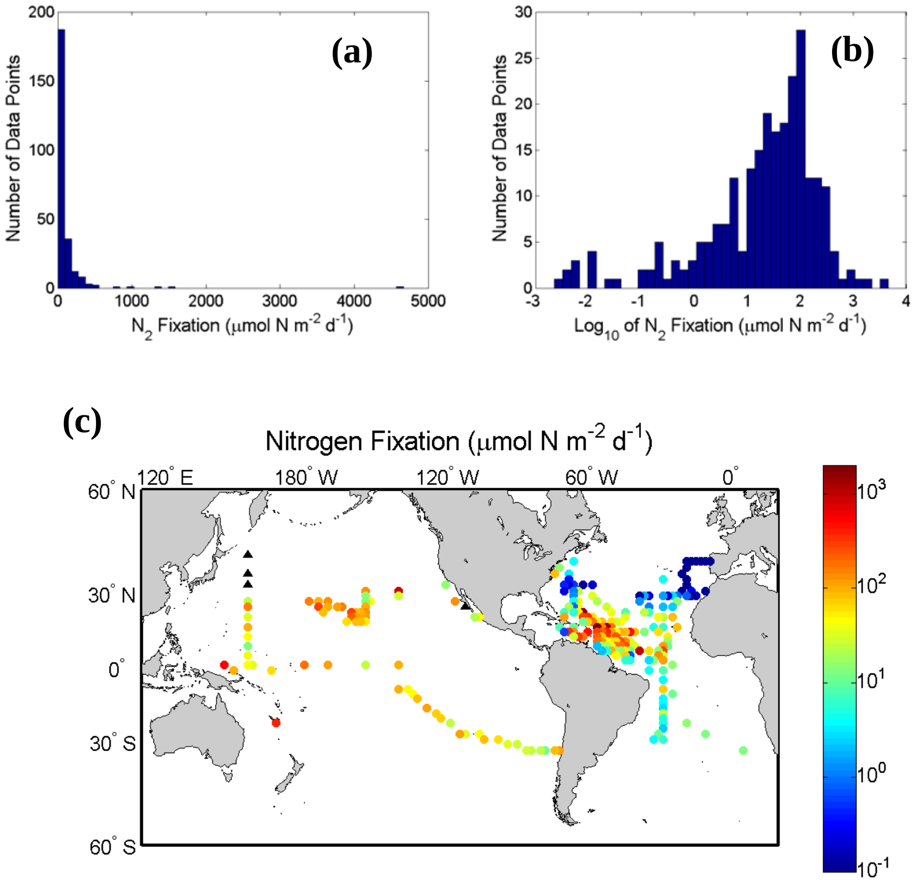

Fig. 1. Histogram of open ocean nitrogen fixation measurements on **(a)** linear and **(b)** logarithmic scales. **(c)** The nitrogen fixation measurements in the Pacific and Atlantic Oceans binned on 2° × 2° grids, with black triangles representing zero nitrogen fixation rates (reported below detection limits).

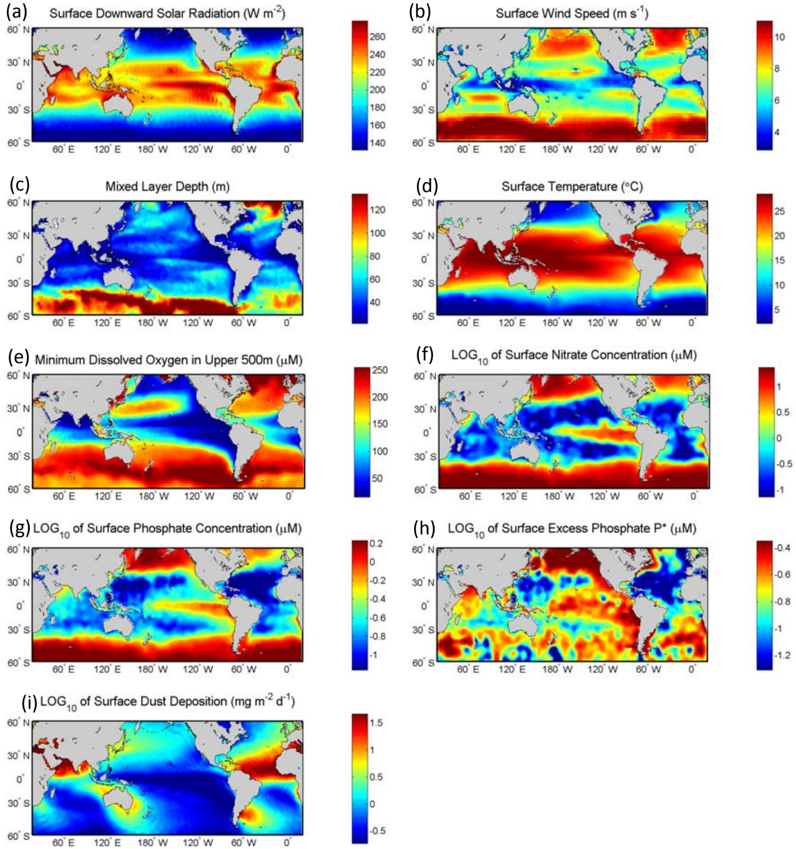

Fig. 2. Maps of environmental parameters in global ocean. Note that nitrate, phosphate, excess phosphate (P^*) and dust deposition are on $\log_{10}$ scale.

BGD
10, 7367–7412, 2013

Environmental controls on marine N_2 fixation

Y.-W. Luo et al.

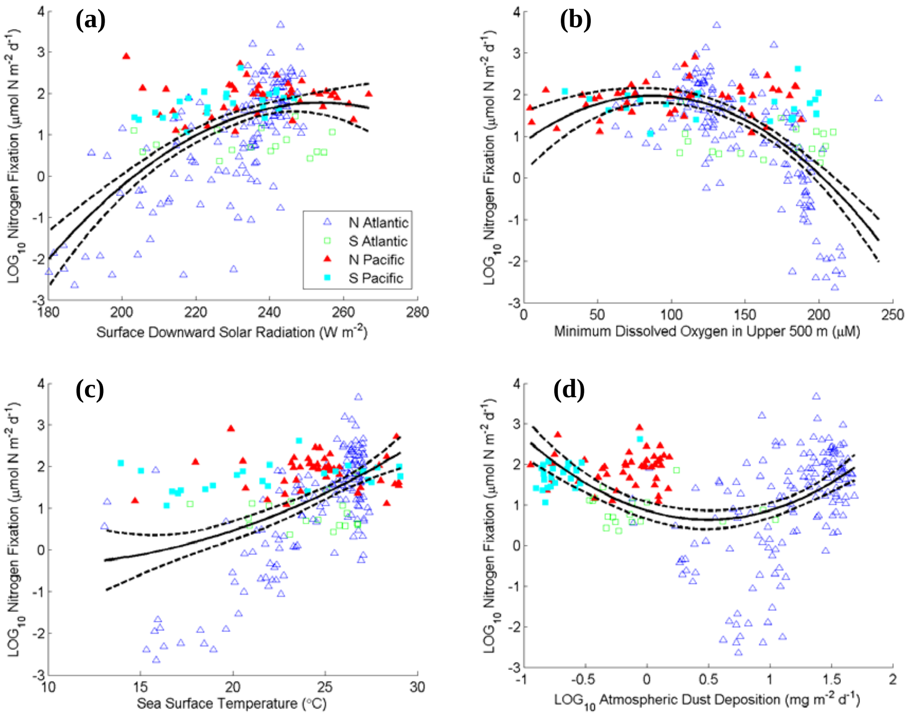

Fig. 3. Quadratic regression (black lines) of log-transformed nitrogen fixation versus **(a)** surface solar radiation, **(b)** minimum dissolved oxygen in upper 500 m, **(c)** sea surface temperature, and **(d)** log-transformed atmospheric dust deposition. The dashed lines represent 95 % confidence intervals for the fitted means.

BGD
10, 7367–7412, 2013

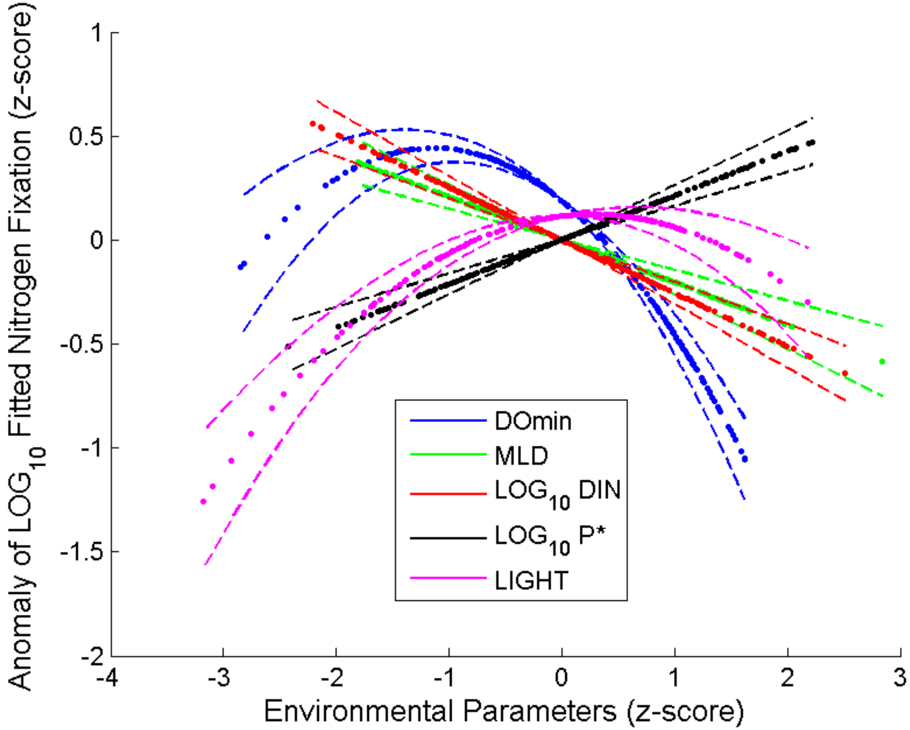

Fig. 4. Final multiple linear regression (MLR) equation, showing functions of fitted log-transformed nitrogen fixation component (anomalies) versus each included predictor, including minimum dissolved oxygen (blue), mixed layer depth (green), log-transformed surface nitrate concentration (red) and excess phosphate (P^*) (black), and surface solar radiation (magenta). The dots are locations of observations and the dashed lines represent one standard error for the fitted means in each component function. Results are standardized (*z*-scores).

BGD
10, 7367–7412, 2013

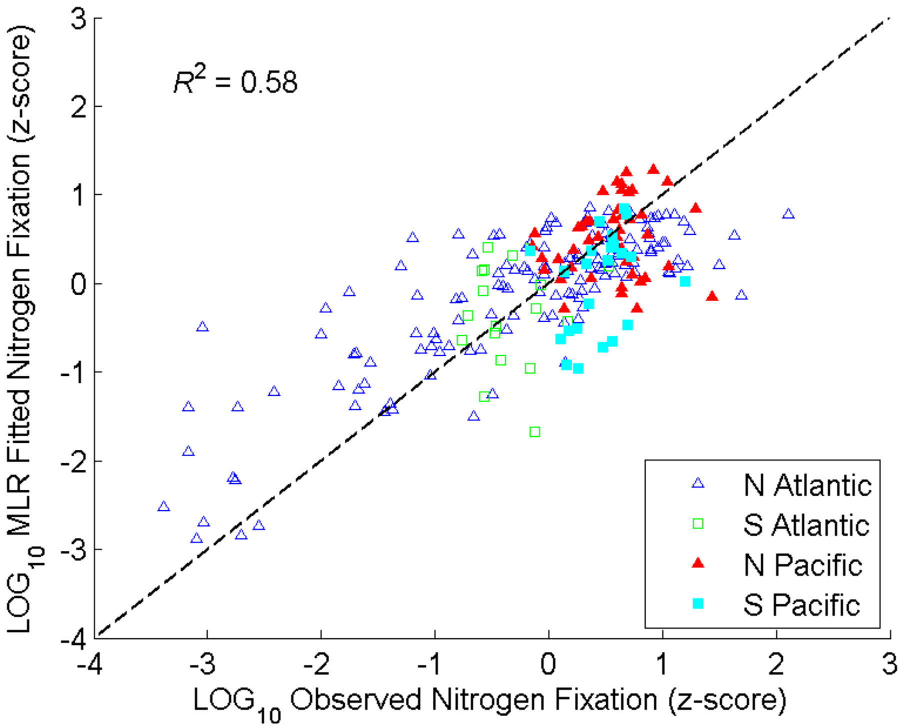

Fig. 5. Final multiple linear regression (MLR) results: observed nitrogen fixation versus MLR-fitted nitrogen fixation. Dashed line is 1 : 1 line. Results were standardized (z-scores).

BGD
10, 7367–7412, 2013

Environmental controls on marine N_2 fixation

Y.-W. Luo et al.

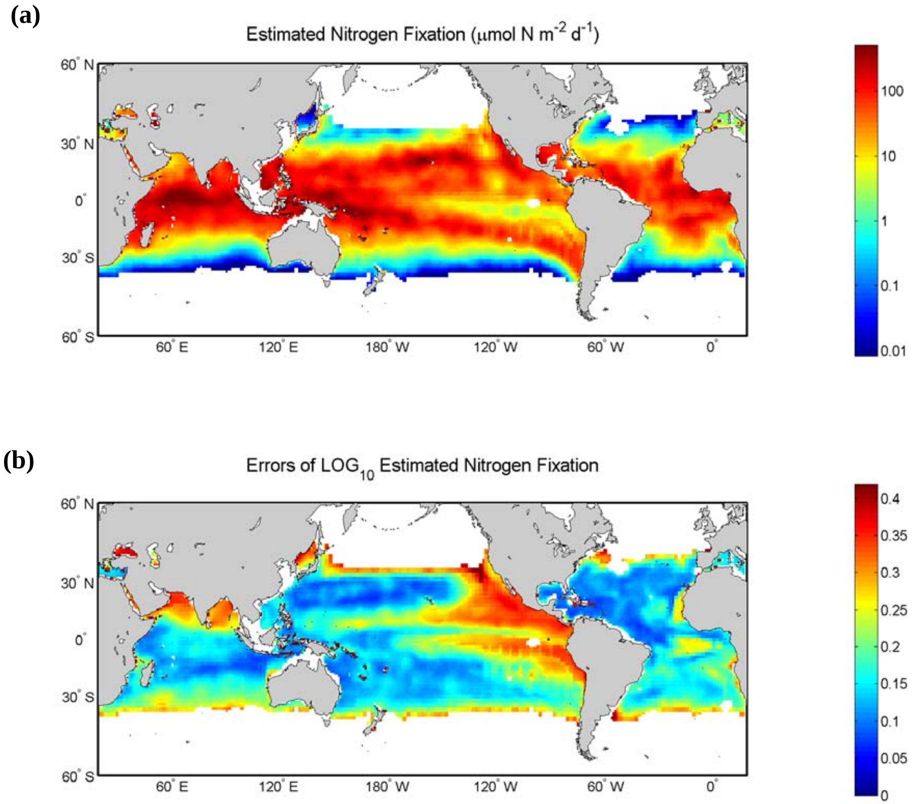

Fig. 6. (a) Map of estimated annual-mean, depth-integrated marine N_2 fixation using equation derived from the multiple linear regression (MLR) and **(b)** the associated errors on $\log_{10}$ scale (see text for details). White areas were outside the limits of the environmental parameter(s) used in the regression or were less than 250 m depth in coastal zones.

BGD
10, 7367–7412, 2013

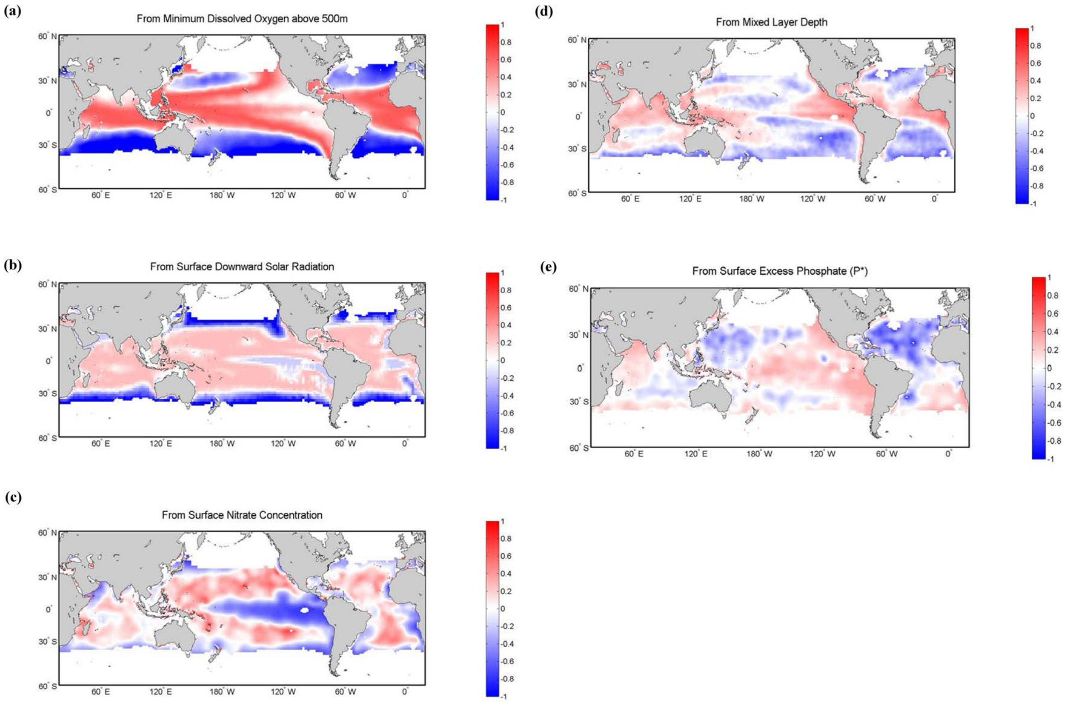

Fig. 7. Anomalies of each predicted component of log-transformed N_2 fixation from environmental parameters including **(a)** minimum dissolved oxygen, **(b)** solar radiation, **(c)** surface nitrate concentration, **(d)** mixed layer depth and **(e)** excess phosphate (P^*). All the panels are plotted on same color scale. In each panel, the vast white areas, approximately north of 40° N and south of 40° S, represent areas where the values of one or more environmental parameters were outside the limits for the MLR used to compute N_2 fixation (see text for details).

BGD
10, 7367–7412, 2013

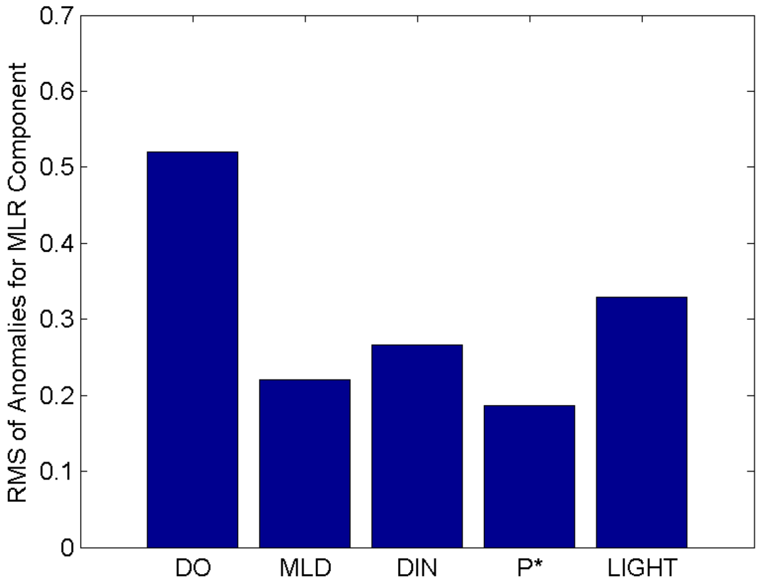

Fig. 8. For the global maps of the anomalies of each predicted $\log_{10}$ N_2 fixation component (those shown in Fig. 7), root mean squares (RMSs) were calculated and compared, including the components predicted from minimum dissolved oxygen (DO), mixed layer depth (MLD), surface nitrate concentration (DIN) and excess phosphate (P^*), and solar radiation (LIGHT).

BGD
10, 7367–7412, 2013

Environmental controls on marine N_2 fixation

Y.-W. Luo et al.